CRYSTAL GROWTH & DESIGN

Article

pubs.acs.org/crystal

Crystal Chemistry in the Barium Fluoride Chloride System

H. Hagemann,*[,†] V. D'Anna,[†] M. Lawson Daku,[†] and F. Kubel[‡]

[†]Department of Physical Chemistry, University of Geneva, 30, quai E. Ansermet, 1211 Geneva 4, Switzerland

[‡]Institut für Chemische Technologien und Analytik, Technische Universität Wien, Getreidemarkt 9/164-SC, A1060 Vienna, Austria

Supporting Information

ABSTRACT: The crystal chemistry of the barium fluoride chloride system is studied both experimentally and theoretically. Different synthetic approaches yield nanocrystalline materials as well as large single crystals. The crystalline phases identified so far are BaFCl, $Ba_{12}F_{19}Cl_5$, and $Ba_7F_{12}Cl_2$ (in two modifications) and are compared with analogous compounds. It is demonstrated that the compound Ba_2F_3Cl reported by Fessenden and Lewin 50 years ago corresponds to $Ba_7F_{12}Cl_2$. The phase diagram of the $BaCl_2$–BaF_2 system is reinvestigated for fluoride mole fractions between 0.5 and 1. The peritectic formation of $Ba_{12}F_{19}Cl_5$ is observed. Periodic density functional theory (DFT) calculations are performed for all structures in this system, including a hypothetical structure for Ba_2F_3Cl, based on the experimental structure of Ba_2H_3Cl. The energy of formation of the different barium fluoride chloride compounds from $BaCl_2$ and BaF_2 (normalized for one barium atom per formula unit), as calculated by DFT at 0 K, is within only about ±15 kJ/mol. Comparison with recent experimental results on calcium and strontium hydride chloride (bromide) compounds suggests the possibility of a mutual exclusion between the M_2X_3Y and $M_7X_{12}Y_2$ (M = Ca, Sr, Ba, Pb, X = H, F, Y = Cl, Br) structures. The single crystal structure of PbFBr is also reported.

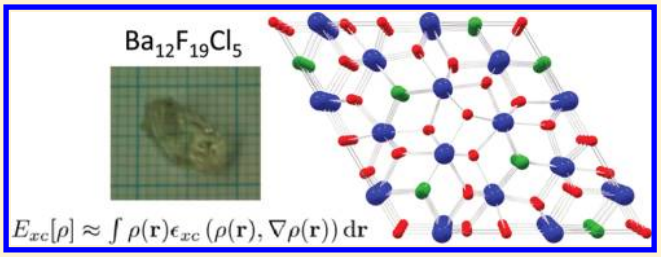

INTRODUCTION

Since the discovery of the potential use of Eu(II)-doped BaFCl and BaFBr as efficient X-ray storage phosphors (ref 1 and references therein), there have been many investigations of the preparation and properties of these and related compounds. For instance, Sm(II)-doped BaFCl crystals are more sensitive pressure sensors than ruby,[2] and room temperature spectral hole burning was performed for the first time in the structurally related Sm^{2+}-doped crystal $SrFCl_{0.5}Br_{0.5}$.[3] The preparation of nanocrystalline BaFCl has been reported recently,[4,5] and when doped with samarium revealed X-ray storage properties.[5,6] Single crystals of $Ba_{12}F_{19}Cl_5$[7] and $Ba_7F_{12}Cl_2$[8] have been prepared and characterized. Eu(II)-doped $Ba_7F_{12}Cl_2$ is an efficient single component white phosphor. In a recent study, Zhang et al[9] reported on "Highly Uniform and Monodisperse Ba_2ClF_3 Microrods: Solvothermal Synthesis and Characterization". Independently and almost simultaneously, Xie et al[10] published a paper entitled "Nucleation and Growth of BaF_xCl_{2-x} Nanorods". In both papers, the same single phase barium fluoro-chloride was prepared and characterized using the 50 year old powder diffraction card (JCPDS No. 07-0029).[11]

Besides the well-known cubic modification of BaF_2, orthorhombic BaF_2 can be obtained under high pressure[12] or by hydrothermal synthesis.[13] Very recently, the preparation of hollow cubic BaF_2 microcubes was presented.[14]

In this paper, we wish to review first the available crystal structure data in the barium-fluoride-chloride system, as well as the crystallochemically related systems barium-hydride-chloride, barium-fluoride-bromide, lead-fluoride-chloride, and lead-fluoride-bromide as well as eventual solid solutions. The single crystal structure of PbFBr is reported. Recent results on other hydrides are also included. We then address some synthetic aspects, related to the preparation of $Ba_7F_{12}Cl_2$ and $Pb_7F_{12}Cl_2$ using different synthetic procedures and compare with the old results by Fessenden and Lewin.[11]

We then investigate the phase diagram between BaFCl and BaF_2 by a combined differential thermal analysis (DTA) and X-ray study. Finally, we present the theoretical structure of the compound Ba_2F_3Cl (based on the experimental structure of Ba_2H_3Cl[15]) using periodic DFT calculations and compare it with the theoretical and experimental structures of $BaCl_2$, $Ba_7F_{12}Cl_2$, BaFCl, and BaF_2 (atmospheric and high pressure phases).

CRYSTALLOGRAPHIC DATA

Table 1 summarizes the compounds in the different systems which have been characterized using single crystal X-ray diffraction. This table shows that with increasing fluoride (hydride) content, the first compounds are the matlockites MFX and MHX; all other compounds have a higher fluoride (hydride) content. The structure of PbFBr was previously refined only from powder diffraction data,[16] a single crystal structure determination was therefore undertaken to complete the available data. The structural parameters agree well with

Received: May 9, 2011
Published: February 15, 2012

   dx.doi.org/10.1021/cg201588s | *Cryst. Growth Des.* 2012, 12, 1124–1131

Table 1. Compounds which Have Been Characterized Using Single Crystal X-ray Diffraction[a]

$BaBr_2$ 15706	BaFBr 2294				BaF_2 64718
$BaCl_2$ 15705	BaFCl 2350		$Ba_{12}F_{19}Cl_5$ 78943	$Ba_7F_{12}Cl_2$ 410679	
	BaHCl 37201	Ba_2H_3Cl 416893			BaH_2 400343
$PbCl_2$ 15806	PbFCl 39165			$Pb_7F_{12}Cl_2$ 10402	PbF_2 14324
$PbBr_2$ 202134	PbFBr 30288			$Pb_7F_{12}Br_2$ 92293	
$SrCl_2$ 28964	SrFCl 2349				SrF_2 41402
	SrHCl 37200			$Sr_7H_{12}Cl_2$ 418948	SrH_2 33160
$SrBr_2$ 15972	SrHBr 25543			$Sr_7H_{12}Br_2$ 418949	
$CaCl_2$ 26158	CaFCl 1130				CaF_2 29008
	CaHCl 25601			$Ca_7H_{12}Cl_2$ 420927	CaH_2 23870
$CaBr_2$ 14220	CaHBr 25542	Ca_2H_3Br 420928			

[a]ICSD numbers are given with each compound.

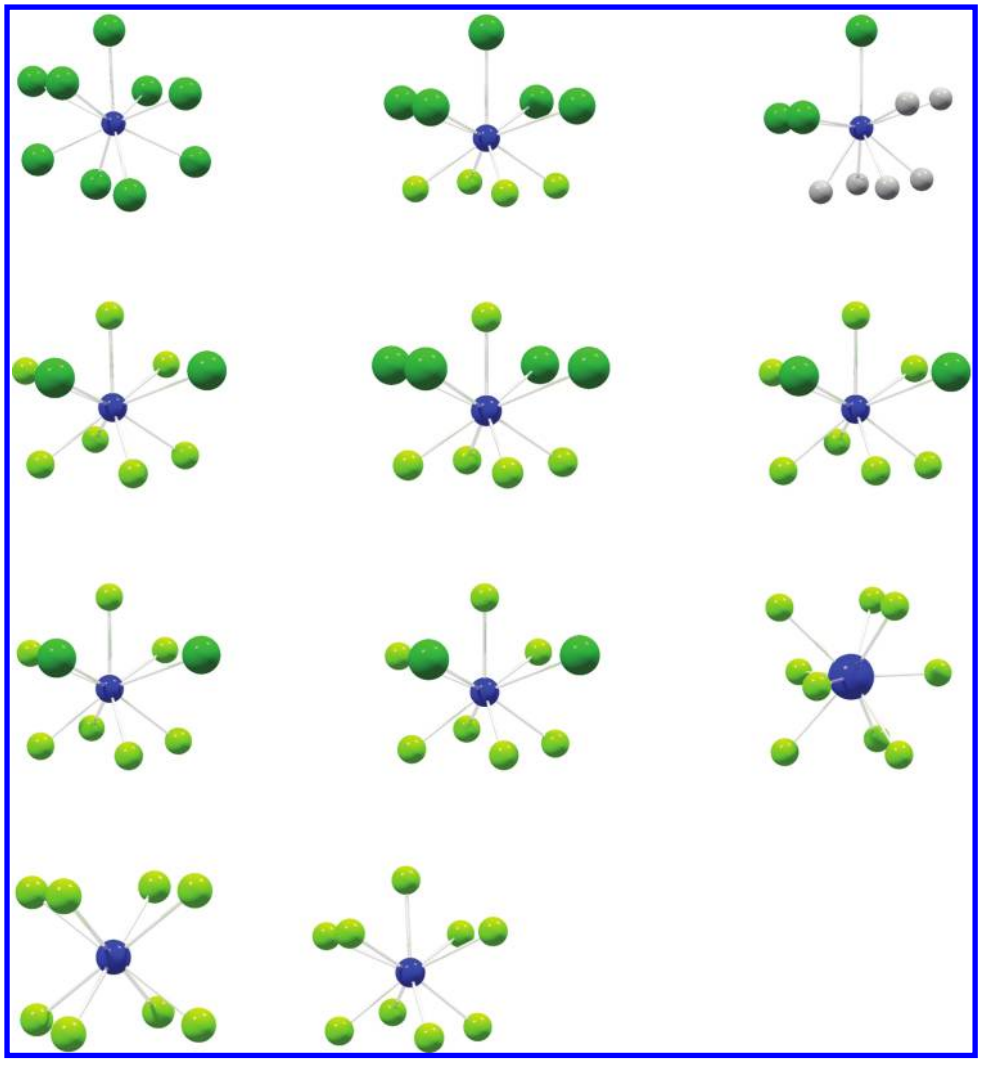

Figure 1. Ba coordination in different crystal structures: blue balls reprepresent Ba, gray balls H, yellow-green balls F, and larger green balls Cl. Top row: $BaCl_2$, BaFCl, Ba_2H_3Cl; second row: Ba(1), Ba(2), and Ba(3) in $Ba_{12}F_{19}Cl_5$; third line Ba(1), Ba(2), and Ba(3) in $Ba_7F_{12}Cl_2$; bottom line BaF_2 (cubic) and BaF_2 (cotunnite).

those of related MFX compounds and are summarized in the Supporting Information.

While the pseudo binary system BaFCl-BaFBr forms solid solutions over the entire composition range,[17] the compounds $Ba_{12}F_{19}Cl_{5(1-x)}Br_{5x}$ and $Ba_7F_{12}Cl_{2(1-x)}Br_{2x}$ form only up to $x \sim 0.6-0.75$.[18,19]

Note however that in the presence of additional metal impurities (Ca, Na) there is a disordered modification of $Ba_{6.33}Ca_{0.67}F_{12}Cl_{2(1-x)}Br_{2x}$ with the value of x ranging from 0 to 1.[20]

The compound BaFCl forms further solid solutions with SrFCl and SrFBr (refs 17 and 21 and references therein). This shows that the matlockite structure is remarkably stable against chemical substitution.

Table 1 shows one structure, namely, $Ba_{12}F_{19}Cl_5$, which appears to have no structural analogue in the other systems.

dx.doi.org/10.1021/cg201588s | Cryst. Growth Des. 2012, 12, 1124–1131

Very recently, the crystal structure of Ca_2H_3Br isotypical to Ba_2H_3Cl was reported.[22] High pressure phases have been reported for BaH_2, BaF_2, and BaFCl.[12,23−25]

Besides the cubic fluorite-type structures of $SrCl_2$ and MF_2 (M = Ca, Sr, Ba), all other compounds shown in Table 1 present at ambient pressure a coordination number (CN) of 9 for the Ba(Pb) atom.

Figure 1 illustrates the coordination observed around Ba in the different crystal structures summarized in Table 1. The 9-fold coordination can be seen

- as a more or less tricapped trigonal prism (as for Ba(3) in $Ba_7F_{12}Cl_2$),
- as a tetragonal complex with a square fluoride basis, then the central Ba atom, then another square rotated by 45 degrees and the ninth ligand atom above (BaFCl, Ba(2) in $Ba_{12}F_{19}Cl_2$), or
- as lower symmetry variants with only two adjacent chlorides in the second plane.

The published phase diagram of the $BaCl_2$−BaF_2 system[26,27] shows only the congruently melting BaFCl compound and two eutectic points (see Figure S1 in the Supporting Information). On the fluoride-rich side, the eutectic point is found at 940 °C for X(F) = 0.73. This phase diagram is very similar to the one reported for the $BaBr_2$−BaF_2 system[28] (see Figure S2). Other phase diagrams of MH_2−MX_2 with M = Ca, Sr, Ba and X = Cl, Br, I also show (Figure S3) the intermediate MHX with the matlockite structure and two eutectic points.[29−31]

In 1955 Fessenden and Lewin[11] reported a compound with composition Ba_2F_3Cl, which was characterized using powder diffraction data that were indexed with a rhombohedral lattice. This compound could be obtained not only by high temperature solid reaction of equimolar amounts of BaF_2 and BaFCl at nominally 900°C, but also by precipitation reactions. The corresponding powder diffraction data were deposited in the JCPDS powder diffraction card no. 07-0029. As will be shown below, this compound corresponds in fact to $Ba_7F_{12}Cl_2$.

EXPERIMENTAL METHODS

Large single crystals (several millimeters) of BaFCl and $Ba_{12}F_{19}Cl_5$ were obtained previously in Geneva using the Czochralski technique,[32,33] both on pure as well as rare earth-doped samples. Other high temperature preparations were done under dry nitrogen atmosphere using dry metal halide powders contained in graphite or glassy carbon crucibles.

Some high temperature experiments were carried out in air, using a Pt crucible.

PbFBr crystals were obtained from a stoichiometric mixture of PbF_2 and $PbBr_2$ by hydrothermal synthesis in Teflon crucibles contained in a stainless steel autoclave at 250 °C for 20 to 60 days.[34]

Low temperature preparations were performed according to a modification of the procedure outlined by Zhang et al,[9] starting from mixtures of oleic acid and water instead of ethanol, with the subsequent addition of soluble barium or lead salts and sodium fluoride, followed by hydrothermal treatment at ca. 160 °C.

Single Crystal Analysis. Single crystals were selected under a polarizing light microscope and optically tested for quality. For X-ray measurements, a Bruker SMART diffractometer with a graphite monochromator and a SMART APEX detector was used. Structure refinements were made using the XTAL[35] program package.

Powder Diffraction. X-ray diffraction measurements were performed on a PANalytical X'Pert PRO system, recently calibrated and optimized using a NIST-LaB_6 standard (emission profile, instrument function, tube tails), with primary and secondary Soller slits of 0.04 rad, a fixed divergence slit of 0.5°, a fixed antiscatter-slit of 1°, and a 200 mm goniometer radius. A standard steel sample holder for flat samples (17 mm Ø) was used. Measuring time was 60 min, 5−135° in 2Θ° with Cu Kα radiation, an X'Celerator detector with Ni Kα filter where the scan length was ca. 2.55°. Refinements were made using the TOPAS 4.2 program package.[36]

DTA Measurements. Caloric measurements were made using a Netzsch STA 449 C Jupiter system in DTA/TG mode with Al_2O_3 crucibles in argon atmosphere. A series of samples with fluoride mole fractions of 0.6, 0.7, 0.73, 0.75, 0.79, 0.84, and 0.9 was prepared from mixtures of previously prepared BaFCl and commercial BaF_2 (Aldrich, 99.999% pure). All samples were heated with a temperature ramp of 20 °C/min to 800 °C, then with a temperature ramp of 5 °C/min from 800 to 1200 °C, back to 800 °C, again to 1200 °C, and back to 800 °C, and finally cooled to room temperature with a temperature ramp of 20 °C/min. Only the data of the second cycle were analyzed, and all samples were subjected to powder X-ray diffraction after the experiment.

DFT Calculations. In order to provide a comprehensive overview of the crystallochemistry in the Ba−F−Cl system, density functional theory (DFT)[37] has been applied to the study of the relative stabilities of the considered crystalline phases. The calculations have performed within the generalized gradient approximation (GGA),[38] using the ABINIT code;[39] the ABINIT code is a common project of the Université Catholique de Louvain, Corning Incorporated, and other contributors (URL http://www.abinit.org), which is based on pseudopotentials and plane waves. It relies on an efficient fast Fourier transform algorithm[40] for the conversion of wave functions between real and reciprocal space, on the adaptation to a fixed potential of the band-by-band conjugate gradient method[41] and on a potential-based conjugate-gradient algorithm for the determination of the self-consistent potential.[42] We used fully nonlocal norm-conserving RRKJ-optimized pseudopotentials[43] generated thanks to the OPIUM code.[44] During the generation of the pseudopotentials, relativistic effects were only taken into account for the heavy Ba atom, for which a scalar-relativistic pseudopotential was actually built.[45] The crystal structures were optimized using 10 × 10 × 10 (BaF_2), 10 × 10 × 5 (BaFCl), 10 × 10 × 5 (Ba_2F_3Cl), 4 × 4 × 12 ($Ba_{12}F_{19}Cl_5$), 10 × 10 × 6 ($Ba_7F_{12}Cl_2$), 6 × 10 × 5 ($BaCl_2$) and 6 × 10 × 5 (BaF_2 high pressure phase) Monkhorst-Pack grids[46] in combination with a kinetic energy cutoff of 40 Ha. Using the optimized structures, phonons were calculated at the center of the Brillouin zone[47] for BaF_2, BaFCl, and Ba_2F_3Cl. The calculations on BaF_2 atmospheric and high pressure phase, $BaCl_2$, BaFCl, Ba_2F_3Cl, $Ba_{12}F_{19}Cl_5$, and $Ba_7F_{12}Cl_2$ were carried out with their symmetries constrained to the space groups $Fm\bar{3}m$, $Pnma$, $Pnma$, $P4/nmm$, $P\bar{3}m1$, $P\bar{6}2m$, and $P\bar{6}$, respectively.

RESULTS AND DISCUSSION

Ba−F−Cl System. In a first step, we tried to reproduce the preparation reported by Fessenden and Lewin.[11] Annealing overnight at nominally 900 °C, a stoichiometric mixture of BaFCl and BaF_2 yielded first a mixture of $Ba_7F_{12}Cl_2$ together with the starting materials; extended annealing over 3 days resulted in the formation of mainly $Ba_{12}F_{19}Cl_5$. Starting from a mixture of $BaCl_2$ + 3 BaF_2 yields a similar result. Further, the powder diffraction data reported by Fessenden and Lewin[11] for the compound "Ba_2F_3Cl" match the powder diffraction data for $Ba_7F_{12}Cl_2$ (ref 48; see also Supporting Information). Careful inspection suggests that two weak lines reported at d = 3.6 and d = 2.20[11] correspond to some BaF_2 impurities. Note also that some intensities reported in the JCPDS No. 07-0029 card do not match those in the original publication[11] (see Supporting Information).

These observations (in conjunction with the other preparations described below) lead to the conclusion that Fessenden and Lewin prepared in fact $Ba_7F_{12}Cl_2$ and not Ba_2F_3Cl.

Single crystal needles (up to several millimeters in length) of $Ba_7F_{12}Cl_2$ ($P\bar{6}$) can be obtained by cooling a mixture containing

BaF_2 and LiCl (typical F mol fraction around 0.85).[8] The melts contains also $LiBaF_3$ and BaF_2. In order to reduce the formation of $LiBaF_3$, mixtures of LiCl and KCl can be used, but also in this case, $LiBaF_3$ and BaF_2 are identified as side products by powder diffraction in the solid, after washing with water.

The use of NH_4Cl as a chloride source (reaction mixture 3 BaF_2 + NH_4Cl, Pt crucible, 850 °C 5 h in air) results in the formation of ca. 80% of $Ba_7F_{12}Cl_2$ in the presence of BaFCl. Changing the ratio of NH_4Cl results in different fractions of BaFCl, $Ba_7F_{12}Cl_2$, and BaF_2, but no other phases were found.

Using NaCl instead of LiCl results in the formation of the disordered modification of $Ba_7F_{12}Cl_2$ (space group $P6_3/m$), which was shown to incorporate small amounts of sodium into the crystal.[49] The optimum F mol fraction was found to be close to 75% (i.e., 2 NaCl + 3 BaF_2). Higher sodium chloride content in the mixture leads to progressively increasing formation of BaFCl.

Previous hydrothermal experiments have resulted in the formation of a superstructure modification of $Ba_7F_{12}Cl_2$.[50]

A new experiment, inspired by the procedure reported in ref 9, using an oleic acid−water mixture for a 1:1 barium chloride/barium bromide solution precipitated by NaF followed by hydrothermal heating at 160 °C for 24 h yielded $Ba_7F_{12}Cl_2$ as textured nanocrystals of 290(6) nm dimensions (estimated from powder diffraction peak width; see Figure 2). Remarkably, the incorporation of bromide is negligible, as can be deduced from the observed lattice parameters.[19]

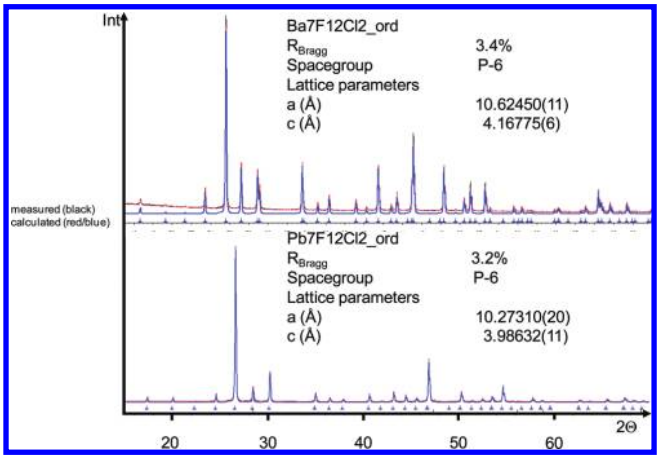

Figure 2. Powder diffraction patterns of different samples: upper trace: $Ba_7F_{12}Cl_2$ from chloride−bromide mixture using the procedure by Zhang[9] (space group $P\bar{6}$, a = 10.6245(1), c = 4.16775(6), R_{Bragg} = 3.4%); lower trace: $Pb_7F_{12}Cl_2$ from hydrothermal synthesis at 220 °C (space group $P\bar{6}$, a = 10.2731(2), c = 3.9863(1), R_{Bragg} = 3.2%.).

In summary, all the experimental results obtained so far indicate only the formation of BaFCl, $Ba_{12}F_{19}Cl_5$, and $Ba_7F_{12}Cl_2$ in addition to the starting materials $BaCl_2$ and BaF_2.

Other Systems. The ordered modification of $Pb_7F_{12}Cl_2$ can also be obtained by hydrothermal methods (see Figure 2). A stoichiometric mixture of lead fluoride and lead chloride and water was subjected to hydrothermal treatment at 220 °C for 10 days yielding single phase $Pb_7F_{12}Cl_2$ as textured small and large needle-shaped crystals with dimensions up to 5 × 0.01 × 0.01 mm (see Figure 3). The preparation of the disordered modification of $Pb_7F_{12}Cl_2$ was previously reported using a NaCl

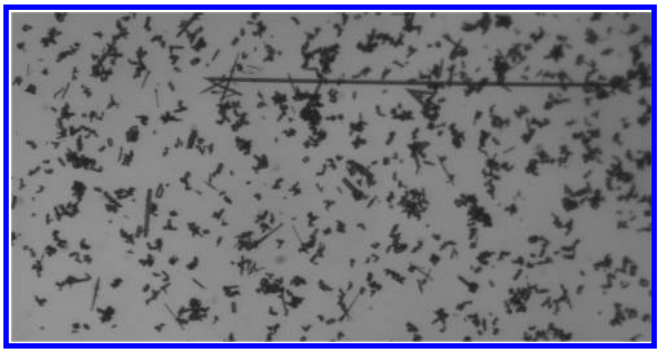

Figure 3. Hydrothermally prepared $Pb_7F_{12}Cl_2$. The length of the long crystal needle is ca. 5 mm.

flux.[51] Larger relative amounts of alkali halide flux lead to the formation of $M_{2x}Pb_{12-x}F_{18}Cl_6$,[52] where M = Na, K.

High temperature solid state reactions between BaF_2 and BaFBr did not form new compounds. However, using alkali chloride-bromide as flux, partially mixed $Ba_7F_{12}Cl_{2-x}Br_x$ has been obtained.[19]

Thermal Analysis and X-ray Study. Figure 4 shows the first derivative of the DTA cooling traces. The onset of the solidification and the eutectic transition are clearly observed. It is important to note that for all samples studied (with a fluoride mole fraction between 0.6 and 0.9), the onset of the eutectic is seen at the same temperature (T = 934 ± 1 °C). In the heating DTA traces, the onset of the eutectic transition is more gradual and found about at about 939 °C, in good agreement with the literature values of 936 °C[26] and 942 °C.[27] Two additional samples, prepared by ball milling, showed a different eutectic temperature, resulting probably from a contamination of the samples during the ball milling process. These data were therefore not considered further.

The corresponding temperatures observed in the heating and cooling runs are collected in Figure 5 and compared with the literature data.[27]

In some heating experiments, a weak DTA signal was observed around 900 °C, but this was not observed in the corresponding cooling run. This peak could be related to the apparently irreversible transformation of $Ba_7F_{12}Cl_2$ (formed by solid state reaction between BaFCl and BaF_2 as seen for the synthesis experiment at 900 °C) to yield $Ba_{12}F_{19}Cl_5$ + BaF_2.

The X-ray analysis of all samples studied by DTA (Figure 6) showed an important amount of $Ba_{12}F_{19}Cl_5$. From the eutectic, one expects only the formation of BaF_2 and BaFCl. The formation of $Ba_{12}F_{19}Cl_5$ is therefore due to a peritectic reaction.

It is important to note that the compound $Ba_7F_{12}Cl_2$ is not observed in these samples. It is not obvious to draw stability boundaries in the solid state between the different phases, as kinetic aspects also come into play. A sample with a fluoride mole fraction of 0.84, heated above the eutectic point and cooled to ca. 800 °C, temperature at which it was left for 15 h, showed again the presence of $Ba_7F_{12}Cl_2$ (11 wt %) together with $Ba_{12}F_{19}Cl_5$ (ca. 55 wt %) and BaF_2 (33 wt %) but practically no BaFCl, in contrast to the samples from the DTA study (see Figure 6). Another sample with a fluoride mole fraction of 0.79 subject to the same treatment did show the presence of $Ba_{12}F_{19}Cl_5$ (ca. 80 wt %), BaFCl (12 wt %), and BaF_2 (8 wt %).

Important amounts of $Ba_{12}F_{19}Cl_5$ are found in the composition range between 70 and 90% of fluoride and show

dx.doi.org/10.1021/cg201588s | *Cryst. Growth Des.* 2012, 12, 1124−1131

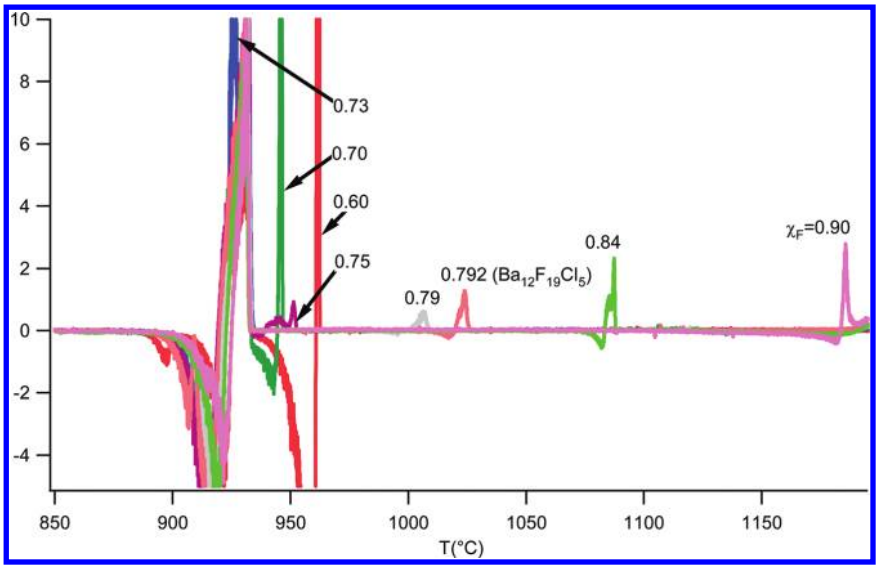

Figure 4. First derivative of the DTA cooling traces.

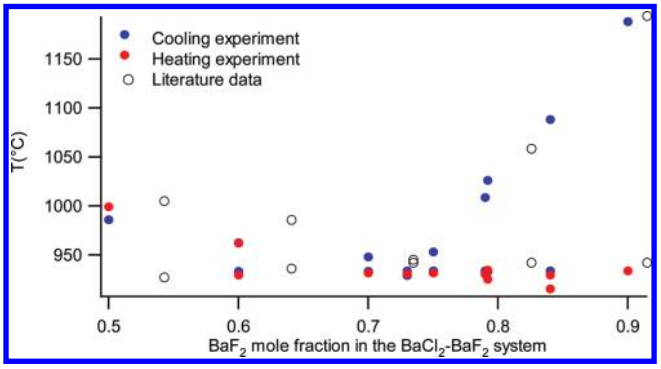

Figure 5. Observed temperatures observed in the heating (red symbols) and cooling (blue symbols) DTA runs. Literature data from ref 27 are shown in black.

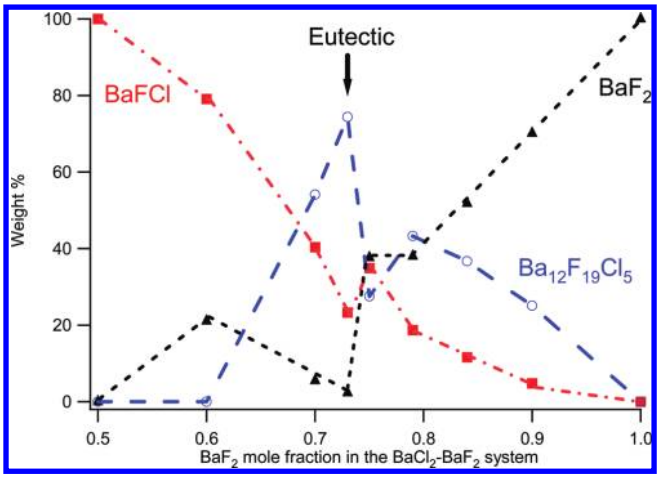

Figure 6. Phase composition of samples after DTA analysis as obtained from Rietvelt refinements of X-ray powder diffraction data.

that this is approximately the stability range for this compound at high temperatures.

Theoretical Calculations. As mentioned above, one expects some crystallochemical similarities between the Ba−F−Cl system and the Ba−H−Cl, Ba−F−Br, and Pb−F−Cl systems. Inspection of Table 1 shows indeed for all systems compounds with the BaFCl structure. The observation of the compounds Ba_2H_3Cl,[15] Ca_2H_3Br,[53] and Sr_2H_3I[54] suggests the possibility to obtain indeed a compound Ba_2F_3Cl. On the basis of the crystal structure of Ba_2H_3Cl, we have optimized the hypothetical structure of Ba_2F_3Cl using periodic DFT (GGA) calculations. It is important to note that the experimental structure of BaH_3Cl[15] has a different space group ($P3\bar{m}1$) than the one reported by Fessenden and Levine[11] (rhombohedral). The detailed calculation procedure (pseudopotentials, grid, etc.) was first optimized for BaFCl against experimental structural and vibrational data.[21] It appears that the proposed structure of Ba_2F_3Cl is stable (i.e., corresponds to a minimum in the potential energy surface; no imaginary vibrational frequencies are calculated at the center of the Brillouin zone), and the structural data for Ba_2F_3Cl are summarized in Table 2.

The coordination around the Ba atom (see Figure 1) shows, in addition to six fluoride atoms, three chloride atoms with slightly larger Ba−Cl bond distances (ca. 3.43 Å) compared to those in the other compounds (3.28−3.40 Å). Note that the calculated bond length in the GGA approximation tend to be slightly overestimated, as can be seen in Table 3 where experimental (taking from the single crystal diffraction data) and theoretical bond lengths are compared.

Further DFT calculations were done for BaF_2, $BaCl_2$, $Ba_{12}F_{19}Cl_5$, and $Ba_7F_{12}Cl_2$ (Tables 2 and 3). With the exception of BaFCl, the calculated unit cell volumes in the GGA approximation are slightly larger than the experimental ones. The lattice parameters of orthorhombic BaF_2 (see Table 2), calculated at ambient pressure, are significantly larger than the experimental parameters (a = 6.159, b = 3.975, and c = 7.853 Å) measured at 4.6 GPa.[12] The unit cell volume (normalized per Ba atom) decreases practically linearly with increasing fluoride content for the theoretical structures with CN 9 (i.e., without cubic BaF_2), in agreement with the experimental structures.[8]

Table 4 summarizes the total energies (in Hartree) calculated for each crystal. These values are divided by N (number of Ba atoms in the unit cell), in order to have the total energy for $BaF_{2y}Cl_{2x}$ for all different values of x and y studied. Using this normalized value of the total energy calculated for each

dx.doi.org/10.1021/cg201588s | Cryst. Growth Des. 2012, 12, 1124−1131

Table 2. Optimized Geometries (at 0 K) and Calculated Total Energies of BaF_2, BaFCl, Ba_2F_3Cl, $Ba_7F_{12}Cl_2$: Results of DFT Calculations Performed at the GGA Level

	space group	cell parameters (Å)	internal reduced coordinates[a]	total energy (Ha)
BaF_2	$Fm\bar{3}m$	$a = b = c = 6.264$	Ba(4a): (0, 0, 0)	−72.411
			F(8c): (1/4, 1/4, 1/4)	
BaF_2	*Pnma*	$a = 6.8068$	Ba(4c): (0.2496, 1/4, 0.1113)	−289.6271
		$b = 4.1150$	F.1(4c): (0.3591, 1/4, 0.4273)	
		$c = 8.0068$	F.2 (4c): (0.9765, 1/4, 0.6643)	
$BaCl_2$	*Pnma*	$a = 8.047$	Ba(4c): (0.2471, 1/4, 0.1113)	−222.969701
		$b = 4.8614$	Cl.1(4c): (0.1417, 1/4, 0.4256)	
		$c = 9.6155$	Cl.2 (4c): (0.0210, 1/4, 0.8356)	
BaFCl	*P4/nmm*	$a = b = 4.460$	Ba(2c): (0, 1/2, 0.2029)	−128.165
		$c = 7.359$	F(2a): (0, 0, 0)	
			Cl(2c): (0, 1/2, 0.6479)	
Ba_2F_3Cl	$P\bar{3}m1$	$a = b = 4.486$	Ba(2d): (1/3, 2/3, 0.7994)	−136.481
		$c = 7.501$	F.1(2d): (1/3, 2/3, 0.1642)	
			F.2(1a): (0, 0, 0)	
			Cl(1b): (0, 0, 1/2)	
$Ba_{12}F_{19}Cl_5$	$P\bar{6}2m$	$a = b = 14.2573$	Ba.1(6k): (0.1671, 0.4747, 1/2)	−827.2718
		$c = 4.3300$	Ba.2(3f): (0.1780, 0, 0)	
			Ba.3(3f): (0.6251, 0, 0)	
			F.1(6k): (0.3630, 0.4889, 1/2)	
			F.2(6j): (0.1824, 0.3760, 0)	
			F.3(3 g): (0.2794, 0, 1/2)	
			F.4(3f): (0.4399, 0, 0)	
			F.5(1a): (0, 0, 0)	
$Ba_7F_{12}Cl_2$	$P\bar{6}$	$a = b = 10.777$	Ba.1(3k): (0.2874, 0.3994, 1/2)	−490.208
		$c = 4.228$	Ba.2(3j): (0.4108, 0.1082, 0)	
			Ba.3(1a): (0, 0, 0)	
			F.1(3k): (0.0481, 0.4368, 1/2)	
			F.2(3k): (0.2148, 0.11933, 1/2)	
			F.3(3j): (0.4301, 0.3664, 0)	
			Cl.1(1f): (2/3,1/3,1/2)	
			Cl.2(1c): (1/3, 2/3, 0)	

[a]The sites occupied by the atoms (Wyckoff positions) are given in parentheses.

compound, it is possible to estimate the reaction enthalpy (at 0 K) for the reaction:

$$x\mathrm{BaCl_2} + y\mathrm{BaF_2} \rightarrow \mathrm{BaF_{2y}Cl_{2x}}$$

by taking the difference between the normalized total energy for a given compound and the normalized energies of $BaCl_2$ and BaF_2 multiplied by x and y, respectively (note that $x + y = 1$).

Accordingly, the theoretical reaction enthalpy to form BaFCl is found to be −15.2 kJ/mol. To the best of our knowledge, no literature data are available, except for a value of the free energy of formation of BaFCl of −992.8 kJ/mol.[55] The literature values of the formation enthalpies and free energies of formation for $BaCl_2$ (−858.6 kJ/mol and −810.3 kJ/mol) and BaF_2 (−1208.8 kJ/mol and −1158.4 kJ/mol respectively)[56] differ both by ca. 50 kJ/mol. Estimating then for BaFCl a formation enthalpy of −992.8 − 50 kJ/mol = −1042.8 kJ/mol, one obtains for the reaction

$$0.5\mathrm{BaCl_2} + 0.5\mathrm{BaF_2} \rightarrow \mathrm{BaFCl}$$

an enthalpy change of about −9 kJ/mol [= −1042.8 − 0.5(−858.6−1208.8)], in reasonable agreement with the theoretical value of −15.2 kJ/mol.

The formation of Ba_2F_3Cl from $BaCl_2$ and BaF_2 is predicted to be endothermic (+9.3 kJ/mol Ba), the formation of $Ba_{12}F_{19}Cl_5$ slightly exothermic (−2.0 kJ/mol Ba) and the formation of $Ba_7F_{12}Cl_2$ slightly endothermic (+0.76 kJ/mol Ba). The formation of the high pressure phase of BaF_2 is also endothermic (11.6 kJ/mol). A recent first principles study of the high pressure phase transitions in BaF_2[57] gives an enthalpy difference of ca. 20 kJ/mol at ambient pressure between the cubic and the cotunnite phases.

In summary, it appears that all theoretical reaction enthalpies remain relatively small (within ±15 kJ/mol). The most exothermic value corresponds to the formation of BaFCl, which is expected as this is the only congruently melting compound besides the starting BaF_2 and $BaCl_2$.

The relative stability of the different compounds can in principle change with temperature, and this is in line with the experimental observation that $Ba_7F_{12}Cl_2$ can be formed by the solid state reaction between BaFCl and BaF_2 (or $BaCl_2$ + BaF_2) between ca. 700 and 900 °C, but transforms to $Ba_{12}F_{19}Cl_5$ and BaF_2 above 900 °C. Thus, in this composition range, we observe at low temperatures mixtures of BaFCl and BaF_2, which start to form $Ba_7F_{12}Cl_2$ above ca. 700 −750 °C which is decomposed at ca. 900 °C to form $Ba_{12}F_{19}Cl_5$.

CONCLUSIONS

In the present work, we have studied experimentally the chemistry of the Ba−F−Cl system and observed the formation of the compounds BaFCl, $Ba_{12}F_{19}Cl_5$, and $Ba_7F_{12}Cl_2$ or mixtures of these together with BaF_2. The unique compound $Ba_{12}F_{19}Cl_5$ (as a similar compound has not been reported so far in the related systems studied here) is formed by a peritectic reaction.

It appears that the compound $Ba_7F_{12}Cl_2$ is relatively stable below 900 °C (above 900 °C, $Ba_{12}F_{19}Cl_5$ is formed). $Ba_7F_{12}Cl_2$ can be prepared using a variety of synthetic approaches in different environments, which suggests that its formation is also kinetically favorable. The relative stability of this structure type is also confirmed by the existence of the analogous compounds $Pb_7F_{12}Cl_2$, $Pb_7F_{12}Br_2$, and $Sr_7H_{12}Cl_2$.[53] Note that this structure type was reported first for phosphides which have been the subject of a recent review.[58] We have shown that it is possible to prepare phase pure $Pb_7F_{12}Cl_2$ using hydrothermal methods.

Periodic DFT calculations suggest that a stable compound Ba_2F_3Cl (based on the structure of Ba_2H_3Cl) may exist. It is less

dx.doi.org/10.1021/cg201588s | Cryst. Growth Des. 2012, 12, 1124−1131

Table 3. Comparison of Experimental (Top, in bold) and Theoretical (DFT-GGA) Ba−F and Ba−Cl Bond Length (Expressed in Å) in the Compounds Studied

	BaFCl	Ba_2F_3Cl	$Ba_{12}F_{19}Cl_5$	$Ba_7F_{12}Cl_2$	BaF_2
Ba−F (min-max)	**2.6481(4)**		**2.5059(6)−3.027(1)**	**2.552(5)−2.965(5)**	**2.663**
	2.6836	2.6044−2.9955	2.6072−3.07095	2.6634−2.8024	2.7125
Ba−Cl (min-max)	**3.206(2)−3.2827(6)**		**3.3155(3)−3.362(2)**	**3.3118(2)−3.3450(2)**	
	3.275−3.3395	3.4277	3.3624	3.4038	

Table 4. Calculated Total Energy for the Different Compounds Studied[a]

compound	*N*: number of Ba atoms in elementary cell	total energy (Hartree)	total energy divided by *N*	$(xBaCl_2 + yBaF_2)/(x + y)$	theoretical reaction enthalpy (Hartree)	theoretical reaction enthalpy (kJ/mol)
$BaCl_2$	4	−222.969701	−55.74242526			
BaFCl	1	−64.08260872	−64.08260872	−64.07681472	−0.005794	−15.2
Ba_2F_3Cl	2	−136.4809641	−68.24048203	−68.24400944	0.00352742	9.3
BaF_2 cubic	1	−72.41120417	−72.41120417			0
$Ba_7F_{12}Cl_2$	7	-4.90×10^2	−70.02966247	−70.02995004	0.00028758	0.76
$Ba_{12}F_{19}Cl_5$	12	-8.27×10^2	−68.93931688	−68.9385419	−0.000775	−2.0
BaF_2	4	−289.6271	−72.40676822		0.00443595	11.6

[a]The theoretical reaction enthalpies (at 0 K) for the reaction $xBaCl_2 + yBaF_2 \rightarrow BaF_{2y}Cl_{2x}$ are given in the last two columns.

stable than BaFCl, $Ba_7F_{12}Cl_2$, and $Ba_{12}F_{19}Cl_5$, but this situation could possibly change under high pressure.

It is important to note that in the different systems studied so far (including Ca and Sr compounds one observes either a compound M_2X_3Y (Ba_2H_3Cl,[15] Ca_2H_3Br,[22] or Sr_2H_3I[54]), or a compound $M_7X_{12}Y_2$ ($Sr_7H_{12}Cl_2$,[53] $Sr_7H_{12}Br_2$,[53] $Ba_7F_{12}Cl_2$, etc.), but not both together.

This suggests that the formation of one or the other compound is probably governed by kinetic properties, leading to a mutual exclusion between the M_2X_3Z and $M_7X_{12}Y_2$ structures.

While this work was in progress, we became aware of a recent thermodynamic evaluation of the Li, Na, K, Mg, Ca, Sr//F, Cl system[59] in which the calculated phase diagram of the SrF_2−$SrCl_2$ system showed good agreement with the experimental data. In this case, similarly to the experimental study of the BaF_2−$BaBr_2$ system,[28] only one mixed fluoride-chloride compound was reported, namely, SrFCl.

■ ASSOCIATED CONTENT

Supporting Information

Single crystal structure data for PbFBr and BaFCl (Table S1), comparison between experimental and theoretical structure data for $Ba_7F_{12}Cl_2$ (Table S2), comparison of powder diffraction data for "Ba_2F_3Cl" and $Ba_7F_{12}Cl_2$ (Table S3), redrawn literature phase diagrams (Figures S1−S5) for the systems BaF_2−BaX_2 (X = Cl, Br), and MH_2 −MX_2 (M = Ca, Sr, Ba, X = Cl, Br, I). This material is available free of charge via the Internet at http://pubs.acs.org.

■ AUTHOR INFORMATION

Corresponding Author

*E-mail: Hans-rudolf.hagemann@unige.ch. Tel + 41 22 379 6539.

■ ACKNOWLEDGMENTS

This work was supported by the Swiss National Science Foundation. We acknowledge supercomputer time at the Swiss National Supercomputing Centre (CSCS) and the Center for Advanced Modeling Science (CADMOS). The authors thank Dr. Jean Claude Grivel and Dr. Béatrice Perrenot for the preliminary DTA data (shown in the Supporting Information). The help of Dr. Christian Gierl for DSC analysis and Mariana Pantazi for the XRD measurements is gratefully acknowledged.

■ REFERENCES

(1) Takahashi, K. *J. Lumin.* **2002**, *100*, 307.
(2) Shen, Y. R.; Gregorian, T.; Holzapfel, W. B. *High Pressure Res.* **1992**, *7*, 73.
(3) Jaaniso, R.; Bill, H. *Europhys. Lett.* **1991**, *16*, 569.
(4) Ju, Q.; Liu, Y.; Li, R.; Liu, L.; Luo, W.; Chen, X. *J. Phys. Chem. C* **2009**, *113*, 2309.
(5) Riesen, H.; Kaczmarek, W. A. *Inorg. Chem.* **2007**, *46*, 7235.
(6) Liu, Z.; Massil, T.; Riesen, H. *Phys. Procedia* **2010**, *3*, 1539.
(7) Kubel, F.; Hagemann, H.; Bill, H. *Z. Anorg. Allg. Chem.* **1996**, *622*, 343.
(8) Kubel, F.; Bill, H.; Hagemann, H. *Z. Anorg. Allg. Chem.* **1999**, *625*, 643.
(9) Zhang, X; Li, C.; Zhang, C.; Yang, J.; Quan, Z.; Yang, P.; Lin. *J. Cryst. Growth Des.* **2008**, *8*, 4564.
(10) Xie, T.; Li, S.; Wang, W.; Peng, Q.; Li, Y. *Chem.—Eur. J.* **2008**, *14*, 9730.
(11) Fessenden, E.; Lewin, S. Z. *J. Am. Chem. Soc.* **1955**, *77*, 4221.
(12) Leger, J. M.; Haines, J.; Atouf, A.; Schulte, O.; Hull, S. *Phys. Rev. B* **1995**, *52*, 13247.
(13) Xie, T.; Li, S.; Peng, Q.; Li, Y. *Angew. Chem., Int. Ed.* **2009**, *121*, 202.
(14) Hou, S.; Xing, Y.; Liu, X.; Zou, Y.; Liu, B.; Sun, X. *Cryst. Eng. Comm.* **2010**, *12*, 1945.
(15) Reckeweg, O.; Molstad, J. C.; Levy, S.; DiSalvo, F. *Z. Naturforsch., B* **2007**, *62*, 23.
(16) Nieuwenkamp, W.; Bijvoet, J. M. *Z. Kristallogr.* **1932**, *81*, 157 (ICSD no. 30288).
(17) Hagemann, H.; Tissot, P.; Lovy, D.; Kubel, F.; Bill, H. *J. Therm. Anal. Calorim.* **1999**, *57*, 193.
(18) Kubel, F.; Hagemann, H.; Bill, H. *Z. Anorg. Allg. Chem.* **1996**, *622*, 1374.
(19) Hagemann, H.; Penhouet, T.; Rief, A.; Kubel, F. *Z. Anorg. Allg. Chem.* **2008**, *634*, 1041.
(20) Frühmann, B.; Kubel, F.; Hagemann, H.; Bill, H. *Z. Anorg. Allg. Chem.* **2004**, *630*, 1484.
(21) D'Anna, V.; Lawson Daku, L. M.; Hagemann, H.; Kubel, F. *Phys. Rev. B* **2010**, *82*, 024108.
(22) Reckeweg, O.; DiSalvo, F. *Z. Naturforsch., B* **2010**, *65*, 493.
(23) Kinoshita, K.; Nishimura, M.; Akahama, Y.; Kawamura, H. *Solid State Commun.* **2007**, *141*, 69.

(24) Smith, J. S.; Desgreniers, S.; Tse, J. S.; Sun, J.; Klug, D. D.; Ohishi, Y. *Phys. Rev. B* **2009**, *79*, 134104.
(25) Subramanian, N.; Chandra Shekar, N. V.; Sahu, P. Ch.; Yousuf, M.; Govinda Rajan, K. *Phys. Rev. B* **1998**, *58*, R555.
(26) Bergman, A. G.; Bukhalova, G. A. *Zhur. Obschei Khim.* **1949**, *19*, 603; *J. Gen. Chem. USSR* **1949**, *19*, 553 (Engl. Translation).
(27) Plato, W. *Z. Phys. Chem.* **1908**, *58*, 350.
(28) Kolb, R.; Schlapp, M.; Hesse, S.; Schmechel, R.; Von Seggern, H.; Fasel, C.; Riedel, R.; Ehrenberg, H.; Fuess, H *J. Physics D: Appl. Phys.* **2002**, *35*, 1914.
(29) Ehrlich, P.; Alt, B.; Gentsch, L. *Z. Anorg. Allg. Chem.* **1956**, *283*, 58.
(30) Ehrlich, P.; Görtz, H. *Z. Anorg. Allg. Chem.* **1956**, *288*, 148.
(31) Ehrlich, P.; Kulke, H. *Z. Anorg. Allg. Chem.* **1956**, *288*, 156.
(32) Nicollin, D.; Bill, H. *J. Phys. C* **1978**, *11*, 4803.
(33) Rey, J. M.; Bill, H.; Lovy, D.; Kubel, F. *J. Phys. Cond. Matter* **1999**, *11*, 7301.
(34) Hagemann, H.; Rief, A.; Kubel, F.; van Mechelen, J. L. M.; Tran, F.; Blaha, P. *J. Phys. Cond. Matter* **2007**, *19*, 036214.
(35) Hall, S. D.; Flack, H. D.; Stewart, G. M., Eds.; *XTAL 3.2 – Users Manual*; Universities of Western Australia, Geneva, and Maryland; Lamb: Perth, 1992.
(36) *TOPAS*, Version 4.2; Bruker AXS GmbH: Karlsruhe, Germany, 2009.
(37) Hohenberg, P.; Kohn, W. *Phys. Rev.* **1964**, *136*, B864. Kohn, W.; Sham, L. J. *Phys. Rev.* **1965**, *140*, A1133.
(38) Perdew, J. P.; Burke, K.; Ernzerhof, M. *Phys. Rev. Lett.* **1996**, *77*, 3865.
(39) Gonze, X.; Beuken, J.-M.; Caracas, R.; Detraux, F.; Fuchs, M.; Rignanese, G.-M.; Sindic, L.; Verstraete, M.; Zerah, G.; Jollet, F.; Torrent, M.; Roy, A.; Mikami, M.; Ghosez, Ph.; Raty, J.-Y.; Allan, D. C. *Comput. Mater. Sci.* **2002**, *25*, 478. Gonze, X.; Rignanese, G.-M.; Verstraete, M.; Beuken, J.-M.; Pouillon, Y.; Caracas, R.; Jollet, F.; Torrent, M.; Zerah, G.; Mikami, M.; Ghosez, Ph.; Veithen, M.; Raty, J.-Y.; Olevano, V.; Bruneval, F.; Reining, L.; Godby, R.; Onida, G.; Hamann, D. R.; Allan, D. C. *Z. Kristallogr.* **2005**, *220*, 558.
(40) Goedecker, S. *SIAM J. Sci. Comput.* **1997**, *18*, 1605.
(41) Payne, M. C.; Teter, M. P.; Allan, D. C.; Arias, T. A.; Joannopoulos, J. D. *Rev. Mod. Phys.* **1992**, *64*, 1045.
(42) Gonze, X. *Phys. Rev. B* **1996**, *54*, 4383.
(43) Rappe, A. M.; Rabe, K. M.; Kaxiras, E.; Joannopoulos, J. D. *Phys. Rev. B* **1990**, *41*, 1227.
(44) http://opium.sourceforge.net
(45) Grinberg, I.; Ramer, N. J.; Rappe, A. M. *Phys. Rev. B* **2000**, *62*, 2311.
(46) Monkhorst, H. J.; Pack, J. D. *Phys. Rev. B* **1976**, *13*, 5188.
(47) Gonze, X. *Phys. Rev. B* **1997**, *55*, 10337.
(48) Kubel, F.; Hagemann, H. *Chem.—Eur. J.* **2010**, *16*, 12526.
(49) Kubel, F.; Hagemann, H. *Cryst. Res. Technol* **2006**, *41*, 1005.
(50) Bernsteiner, A.; Kubel, F. *Acta Crystallogr. C* **2006**, *62* (6), i41–i42.
(51) Kubel, F.; Hagemann, H.; Bill, H. *J. Solid State Chem.* **2000**, *149*, 56.
(52) Kubel, F.; Rief, A. *Z. Kristallogr.* **2006**, *221*, 600.
(53) Reckeweg, O.; Molstad, J. C.; Levy, S.; Hoch, C.; DiSalvo, F. J. *Z. Naturforsch. B* **2008**, *63*, 513.
(54) Reckeweg, O.; DiSalvo, F. *Z. Naturforsch. B* **2011**, *66*, 21.
(55) Moore, D. J. *J. S. Afr. Chem. Inst.* **1970**, *23*, 125.
(56) Chase, M. W., Jr. NIST-JANAF Thermochemical Tables, 4th ed.; *J. Phys. Chem. Ref. Data, Monograph 9*, **1998**, 1–1951.
(57) Yang, X; Hao, A.; Wang, X; Liu, X.; Zhu, Y. *Comput. Mater. Sci.* **2010**, *49*, 530.
(58) Jeitschko, W.; Meisen, U.; Albering, J. *Dalton Trans.* **2010**, *39*, 6067.
(59) Renaud, E.; Robelin C., E.; Gheribi, A. E.; Chartrand, P. *J. Chem. Thermodyn.* **2011**, *43*, 1286.